Available online at www.sciencedirect.com
SCIENCE DIRECT®
Journal of Colloid and Interface Science 273 (2004) 331–338
JOURNAL OF Colloid and Interface Science
www.elsevier.com/locate/jcis

Controlling the transport of cations through permselective mesoporous alumina layers by manipulation of electric field and ionic strength

Riaan Schmuhl, Klaas Keizer, Albert van den Berg, Johan E. ten Elshof,* and Dave H.A. Blank

Inorganic Materials Science, MESA+ Institute for Nanotechnology & Faculty of Science and Technology, University of Twente, P.O. Box 217, 7500 AE, Enschede, The Netherlands

Received 14 July 2003; accepted 22 October 2003

Abstract

The electric field-driven transport of ions through supported mesoporous γ-alumina membranes was investigated. The influence of ion concentration, ion valency, pH, ionic strength, and electrolyte composition on transport behavior was determined. The permselectivity of the membrane was found to be highly dependent on the ionic strength. When the ionic strength was sufficiently low for electrical double-layer overlap to occur inside the pores, the membrane was found to be cation-permselective and the transport rate of cations could be tuned by variation of the potential difference over the membrane. The cation permselectivity is thought to be due to the adsorption of anions onto the pore walls, causing a net negative immobile surface charge density, and consequently, a positively charged mobile double layer. The transport mechanism of cations was interpreted in terms of a combination of Fick diffusion and ion migration. By variation of the potential difference over the membrane the transport of double-charged cations, Cu^{2+}, could be controlled accurately, effectively resulting in on/off tunable transport. In the absence of double-layer overlap at high ionic strength, the membrane was found to be nonselective.

Keywords: Permselectivity; Transport; Mesoporous; Alumina; Membrane; Double layer

1. Introduction

In recent years a significant number of works have appeared that deal with the development of switchable interconnects with which certain species from fluids can be transported at will across a semipermeable barrier [1,2]. The development of selective barriers that allow active control over the transport of specific molecular or ionic species may ultimately lead to new intelligent interconnects between fluid channels in microchemical systems (MiCS) and micrototal analysis systems (μTAS) [3,4]. The ability to move molecules with high precision, selectivity, and temporal control may result in smaller devices, lower power consumption, and improved accuracy. Materials with switchable molecular functions may lead to completely new approaches to valves, chemical separation, and detection.

One of the pioneering works in this field was performed by Martin and co-workers, who showed that the permselectivity of Au-coated track-etched nanotubular membranes can be controlled by manipulation of the membrane electrical potential relative to the potential in the feed [5]. Essentially, the membrane surface was charged relative to the solution bulk, and as the pores were sufficiently small for the double layer to penetrate the entire pore diameter, an ion-selective membrane was obtained. When the membrane surface was negatively charged, predominantly cationic fluxes were observed, and vice versa [5].

Two factors are of prime importance to control the transport of species through a barrier actively, namely permselectivity and driving force. The occurrence of permselectivity in mesoporous oxide thin layers towards cations or anions depends on the thickness of the double layer relative to the pore radius, the magnitude and sign of the interior surface charge, and the surface charge at the solution–membrane interface [2]. High selectivity toward either cations or anions will occur when the ionic double-layer spans the membrane pores, i.e., when the double-layer thickness is larger than the pore radius a [2,6]. The double-layer thickness can be estimated from the Debye length κ^{-1} [7],

* Corresponding author.
E-mail address: j.e.tenelshof@utwente.nl (J.E. ten Elshof).

0021-9797/$ – see front matter
doi:10.1016/j.jcis.2003.10.024

$$\kappa^{-1} = \sqrt{\frac{\varepsilon_0 \varepsilon_r k_B T}{e^2 \sum_i z_i^2 n_i^0}}, \tag{1}$$

where e is the elementary electron charge, ε_0 the permittivity of vacuum, ε_r the relative permittivity of the liquid medium, k_B the Boltzmann constant, T the temperature, z_i the charge of ion species i, and n_i^0 the number density of ion species in the bulk of the electrolyte solution [7]. The double-layer thickness is not constant but decreases with ionic strength and increases with surface charge density [8].

When $\kappa a < 1$, the dimensions of narrow-sized channels approach the length of the double layers and overlap occurs from opposite sides. Under these conditions of complete double layer overlap the channel becomes virtually impermeable to ions with the same charge as the surface charge, thus making it a selective barrier for transport of either cationic or anionic species. Alternatively, under conditions at which $\kappa a > 1$, the double layer is confined to a small region near the channel wall; the center of the channel is electrically uncharged. Under these conditions both cationic and anionic species can be transported through the channel [7].

This principle has been used by Bluhm et al. to demonstrate the correlation between cation permselectivity and external conditions [9]. They investigated the diffusion of cations across mesoporous Anopore γ-alumina membranes as a function of pore diameter, pH, and ionic strength. They concluded that at low ionic strength the alumina surface charge and the large Debye length dominate the cation permeability. This effect was observed for 20-nm pores with a salt solution of $\leqslant 10^{-4}$ M, at which concentration the electrical double-layer thickness is on the order of several tens of nanometers. By increasing the salt concentration the Debye length should diminish, allowing the bulk solution to penetrate into the pores [9].

A driving force for species transport across a membrane can be obtained by applying an external electric field over the membrane. By controlling the dimensions of the electrical double layer relative to the pore diameter and the magnitude and sign of the applied potential, the transport of charged and uncharged species through nanoporous media over micrometer length scales may be spatially and temporally manipulated. Kemery et al. investigated the effect of electric field on the mass transport of cationic, anionic, and neutral species through polycarbonate tracked–etched membranes [2]. They concluded that the permeability response to the electric field depended on the molecular charge and electrolyte concentration. They also found that anions were physisorbed on the internal channel walls, which produced a largely immobile negative charge density, which in turn led to a predominantly cationic mobile double layer to mediate transport in the channel [2].

Hence, a combination of double-layer overlap and the external driving force (electric field) provides a way to tune the transport rate of either anions or cations from one side of the barrier to the other. By placing the electrodes very close together, or even attaching them on both sides of the selective barrier, it is possible to generate reasonably large fields without danger of electrochemical decomposition of valuable species. However, in the latter mode of operation the electrodes will generate bias potentials relative to the bulk solutions with which they are in contact, so that an external double layer, in which ions are accumulated or depleted with respect to the bulk concentrations of the solutions, is generated outside the membrane. In general, the local concentration c_i^{int} of an ion of type i near such an interface will deviate from its concentration c_i^{bulk} in the bulk solution under the influence of a (small) bias potential, ΔV_{bias}, according to the equation

$$c_i^{\text{int}} = c_i^{\text{bulk}} \exp\left(-\frac{z_i e \Delta V_{\text{bias}}}{k_B T}\right). \tag{2}$$

If z_i is positive, a negative ΔV_{bias} will cause cations to accumulate near the interface, while a positive ΔV_{bias} will have the reverse effect [7].

We will demonstrate this principle in this paper and show that high tunability of flux can be achieved, using a γ-alumina membrane and Cu^{2+} ions as model membrane and species, respectively. The transport of ionic and neutral species through charged γ-alumina membranes mediated by a variable external electric field can be regarded as a model system for some of the types of applications mentioned earlier [2,6]. Due to the small pore sizes of typically ∼5 nm in the γ-alumina layer and the amphoteric surface charge that is present on the internal pore walls, partial or complete overlap of a negatively or positively charged diffuse double layer may occur inside the pores, depending on the total ionic strength [2] and pH [9]. This may make γ-alumina a predominantly anion-, cation-, or nonselective barrier depending on externally tunable parameters. Further control over the transport of species is obtained by application of an external electric field over a membrane via gold electrodes that are attached to both sides of the membrane [2,5]. In the present study the influence of electrolyte type, ionic strength, and dc potential difference on the transport rates of ions and neutral solutes through a stacked Au/α-Al_2O_3/γ-Al_2O_3/Au membrane is investigated.

2. Experimental

2.1. Materials

Deionized H_2O (18.2 MΩ cm) from a Milli-Q water purification system (Millipore) was used to prepare all solutions. Commercially available reagents were used without further purification. AKP 30 powder was obtained from Sumitomo chemicals. Aluminum tri-*sec*-butoxide (ATSB), $CuCl_2$, $Cu(NO_3)_2$, KCl, KNO_3, NaOH, and HNO_3 were obtained from Merck. KF was obtained from Aldrich and *d*-tryptophan from Fluka.

2.2. Membranes

The membranes consist of two components: a macroporous support and a thin mesoporous layer with a separative ability. α-Alumina is used as macroporous support and coated with mesoporous γ-alumina layers. The method of preparation of the α-alumina support is so-called colloidal filtration. A colloidal suspension was made by dispersing 50 wt% α-alumina powder (AKP 30) in 0.02 M nitric acid solution using ultrasonic treatment for 15 min. The suspension was filtered over polyester filters (pore size 0.8 µm). The resulting filter cake was dried overnight and fired at 1100 °C for 1 h. After firing, the supports were machined to the required size and polished [10]. The γ-alumina membranes were prepared by dip-coating the sintered α-alumina supports in a homemade boehmite sol. The boehmite sol was prepared by a colloidal sol–gel route, where aluminum tri-*sec*-butoxide (ATSB) was hydrolyzed and subsequently peptized with HNO_3 [10]. The boehmite sol was mixed with a PVA solution, in a PVA:boehmite mass ratio of 2:3. Dip coating was preformed under class 1000 clean room conditions in order to minimize particle contamination of the membrane layer. After dipping, the membranes were dried in a climate chamber at 40 °C and 60% R.H. to avoid crack formation in the boehmite layer. γ-Alumina membranes were formed by firing the dried layers at 600 °C for 3 h in air. Laterally conductive macroporous gold layers were sputtered on both sides of the α/γ-alumina composite membrane at room temperature.

2.3. Permporometry

The permporometry technique [11] was used to determine the average pore size and pore size distribution of the membranes. Permporometry is based on the controlled blocking of the pores by capillary condensation and the simultaneous measurement of the gas diffusion flux through the remaining open pores. When a condensable vapor (cyclohexane) is introduced at low vapor pressure, first a molecular adsorption layer (the so-called "t-layer") is formed on the inner surface of the pores. When the relative vapor pressure P/P_0 of the condensable gas is increased further from zero to unity, pores with increasingly large radius become blocked due to capillary condensation. The simultaneous gas flux through the remaining open pores provides a measure for the fraction of pores with pore size larger than the pores that are already blocked. Upon desorption the same processes occur in reverse order. The relationship between relative vapor pressure and the capillary condensation of pores with Kelvin radius r_K upon desorption is given by the equation

$$\ln(P/P_0) = -\frac{2\gamma_s V_m}{r_K RT}, \tag{3}$$

where γ_s and V_m are the surface tension and molar volume of the condensable gas, respectively, R is the gas constant, and T the temperature.

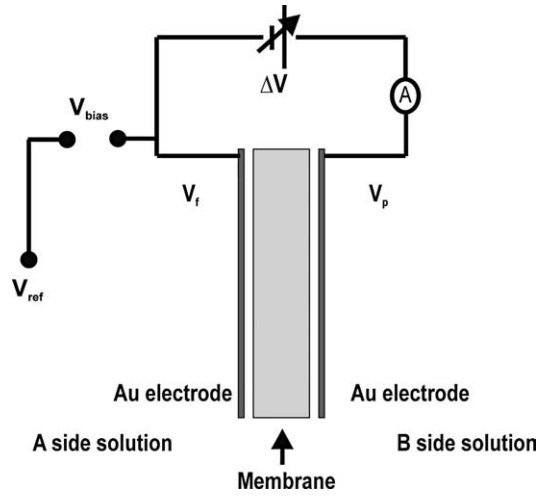

Fig. 1. Schematic diagram of the experimental setup for transport experiments.

The relationship between the real pore width (d_p) and the Kelvin radius (r_K) is given by the equation

$$d_p = 2(r_K + t), \tag{4}$$

where t is the thickness of the "t-layer" formed on the inner surface of the pores, which is usually 0.3–0.5 nm. A more detailed description of the permporometry setup can be found in the article of Cao et al. [11].

2.4. Transport experiments

The experimental setup is schematically depicted in Fig. 1. The membrane was placed between the two halves of a U-shaped tube with the γ-alumina layer exposed to the so-called A side of the membrane (surface area 3.3 cm^2). Aqueous electrolyte solutions (500 ml volume) were added to the A and B side cells and stirred vigorously. The pH was regulated with NaOH or HNO_3 solutions. A dc potential difference ΔV was imposed [6] using a potentiostat. Here ΔV is defined as $\Delta V = V_B - V_A$, with V_A and V_B the electrode potentials at the A and B side, respectively. ΔV was typically kept between -0.5 and $+0.5$ V to prevent Cu reduction. The bias potential $\Delta V_{bias} = V_A - V_{ref}$ between the electrode and the A-side solution was monitored with an Ag/AgCl reference electrode. All experiments were performed at room temperature. The ion concentrations were analyzed by atomic absorption spectroscopy (Thermo-Optec BV SOLAAR System 939) for Cu^{2+} and ion chromatography (Dionex 120) for K^+, Na^+, Cl^-, F^-, and NO_3^-. The ion fluxes were calculated from the concentration changes with time after reaching steady-state conditions. Prior to the experiment the membranes were left for 12 h in the B-side electrolyte solution to ensure complete wetting. Electro-osmotic flow (EOF) measurements were carried out by adding 8 mM d-tryptophan to the A side and monitoring the concentration change at the B side by a BMG Floustar$^+$ (Model 403) microplate reader at the excitation (emission) maximum of 289

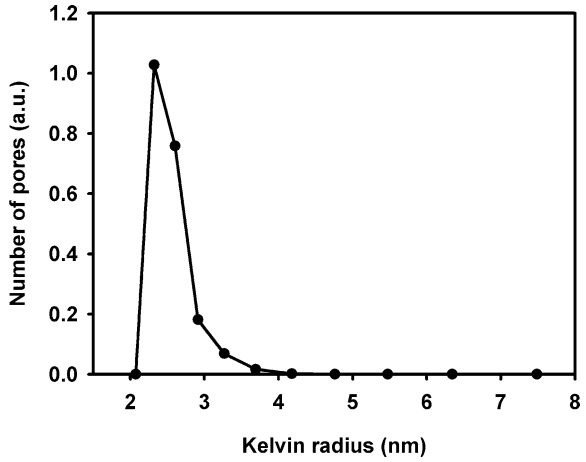

Fig. 2. Pore size distribution of γ-Al_2O_3 layer, as measured by permporometry.

(366) nm. The detection limit of *d*-tryptophan was determined to be 0.5 µM. The pH was regulated with a phosphate buffer at pH 6.9 after the imposition of a dc potential difference ΔV between -0.5 and $+0.5$ V. X-ray photoelectron spectroscopy (XPS) analysis on membrane fragments was done with a PHI Quantum 2000 scanning X-ray microprobe.

3. Results and discussion

3.1. Characterization

The support has a thickness of 2 mm, a pore size of 80–100 nm, and a porosity of ∼30% [12]. The γ-alumina layer is ∼1 µm thick and has a porosity of 40–50% as described elsewhere [12]. The pore size distribution of the γ-alumina layer supported on α-alumina as determined by permporometry are shown in Fig. 2. There is a sharp increase in the number of pores around a Kelvin radius of 2.5 nm using Eq. (3), which corresponds to pore sizes in the range of 4.5–7.5 nm. The technique was also used to check for the absence of defects >8 nm in the γ-Al_2O_3 layer.

3.2. Transport phenomena

The transport of water-soluble neutral, anionic, and cationic species under the influence of a variable electric field over the mesoporous alumina membrane was investigated as a function of different parameters, such as concentration, pH, and electrolyte type. The absolute values of fluxes were found to differ slightly from one membrane to another; however, the general trends were reproducible. The electrolyte bulk concentrations in all experiments correspond with Debye lengths κ^{-1} in the range of 3–11 nm, unless stated otherwise. Since r_K is 2.0–3.5 nm, it is expected that complete double-layer overlap occurs inside the γ-Al_2O_3 layer. Fig. 3 shows the concentration of Cu^{2+} at the B side versus time after the start of the experiment and at

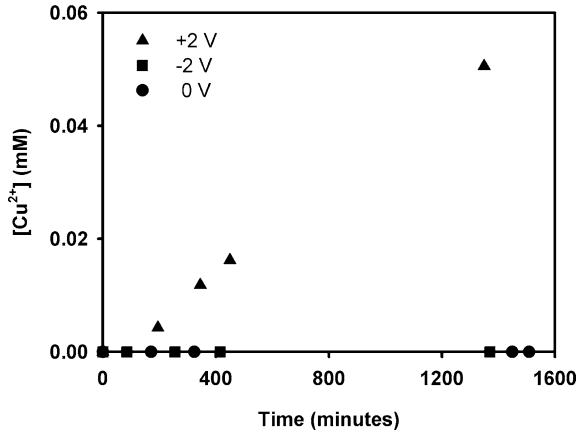

Fig. 3. Plots of Cu^{2+} ions transported to the B side with time at indicated potential differences ΔV. pH = 5.5. Initial concentrations: $[Cu(NO_3)_2] = 1.33$ mM (A), [KF] = 0.86 mM (B).

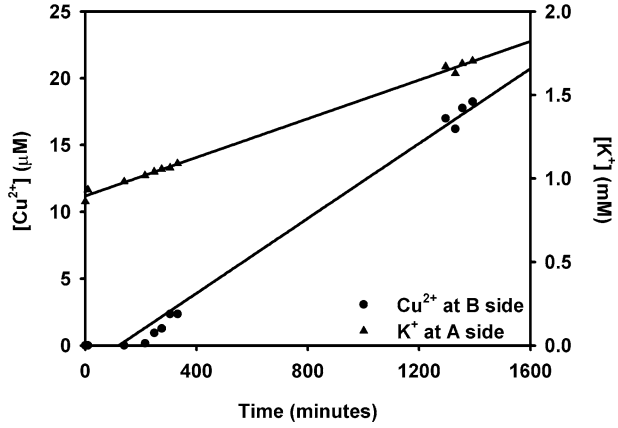

Fig. 4. Concentration changes of K^+ at the A side and Cu^{2+} at the B side with time. $\Delta V = 2$ V; $\Delta V_{bias} = -24$ mV; $i = 1.0$ mA/cm^2; pH = 5.6. Initial concentrations: $[Cu(NO_3)_2] = 2.67$ mM (A), [KF] = 0.86 mM (A), [KF] = 0.86 mM (B). Drawn lines serves as a guide to the eye.

various potential differences ΔV over the membrane. When ΔV was positive, Cu^{2+} ions were transported across the membrane, but under field off and at negative ΔV no transport of Cu^{2+} occurred. The electrolyte compositions were different on the A and B sides of the membrane, so that the transport of all species could be monitored easily. Although the electrolyte strengths on both sides were similar, they were not exactly the same. This leads to a small osmotic pressure difference $\pi = RT\,\Delta c$ between the two membrane sides (Δc is the ion concentration difference), but since π is typically <0.1 bar, the effect is considered negligible in comparison with the driving force exerted by the electrical field [13]. By varying the potential difference over the membrane no significant changes in the concentration of anions (NO_3^- and F^-) at the A or B sides were observed, while transport of K^+ and Cu^{2+} did occur.

Fig. 4 shows the effect of a positive potential difference over the membrane on the transport of ions. Immediately after the start of the experiment a linear increase of the K^+ concentration on the A side of the membrane with time

could be observed. The K^+ accumulation corresponded to a steady K^+ flux of $(1.44 \pm 0.05) \times 10^{-5}$ mol/m^2 s. After about 140 min a Cu^{2+} flux of $(3.7 \pm 0.1) \times 10^{-7}$ mol/m^2 s in the opposite direction developed. No significant changes in the concentrations of NO_3^- and F^- could be observed during the course of the experiment. To check for the absence of anion transport, a number of other anions including Cl^- and MnO_4^- were also investigated, but irrespective of pH and applied potential difference, no anion transport was observed in any experiment. These results suggest that the γ-alumina membrane has a high permselectivity towards cations.

In all experiments the current was also measured. The Au electrodes were found to be stable, as atomic absorption spectroscopy (AAS) analysis did not show any Au present in the A- or B-side solutions after the experiments. No gas evolution was detected at the electrodes. Therefore, the main electrode reactions occurring are thought to be the oxidation and reduction of H_2O at underpotential.

In general, the imposed potential difference will induce an electrokinetic flow, so that all ion fluxes are due to one or more of three contributions: (1) electro-osmotic flow, which is driven by the mobile double layer inside the pores and moves the entire liquid under the influence of an electric field gradient, (2) ion migration, which moves charged species toward the oppositely charged electrode, and (3) diffusion, which moves both charged and uncharged species under the influence of a concentration gradient [2]. EOF experiments were carried out using typical electrolyte solutions containing *d*-tryptophan as a neutral probe molecule, but it was established that this mode of transport does not contribute significantly to the observed fluxes up to field strengths of at least $\pm 10^3$ V/m ($|i| < 1.2$ mA/cm^2).

In the experiment shown in Fig. 4 the net K^+ flux was directed from the positive to the negative electrode while no concentration gradient was initially present. Hence, in this case the K^+ flux must be attributed to ion migration. In contrast, the Cu^{2+} fluxes cannot be explained by the same mechanism, since they were always directed towards the positively charged electrode at low ionic strength. One possible explanation for the observed Cu^{2+} flux could be surface diffusion, since divalent metal cations are known to diffuse over the interior membrane surface [14]. However, the typical surface diffusion coefficients ($\sim 10^{-12}$ m^2 s^{-1}) for this process are too small to explain the magnitude of the observed Cu^{2+} flux entirely [14]. Normal Fick diffusion of solvated Cu^{2+} species will probably contribute much more to the observed flux, but this does not explain the ΔV dependence of the Cu^{2+} flux that is shown in Fig. 4. The latter effect will be explained later.

3.3. Influence of feed concentration and pH

The influence of the Cu^{2+} concentration on flux is shown in Fig. 5. The flux of Cu^{2+} increased with increasing feed concentration at constant ΔV and pH, although not linearly. It was found that the flux of Cu^{2+} also varied with pH at

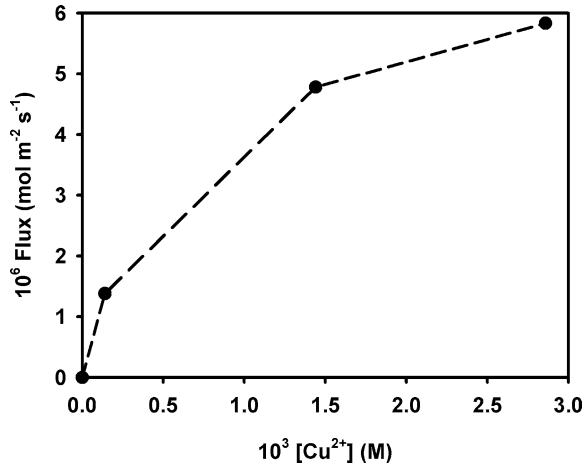

Fig. 5. Cu^{2+} flux versus initial copper concentration. $\Delta V = 1$ V; pH 6.5; $[CuCl_2] = 0.14$, 1.4, and 2.9 μM (A); [KCl] = 1.34 mM (B).

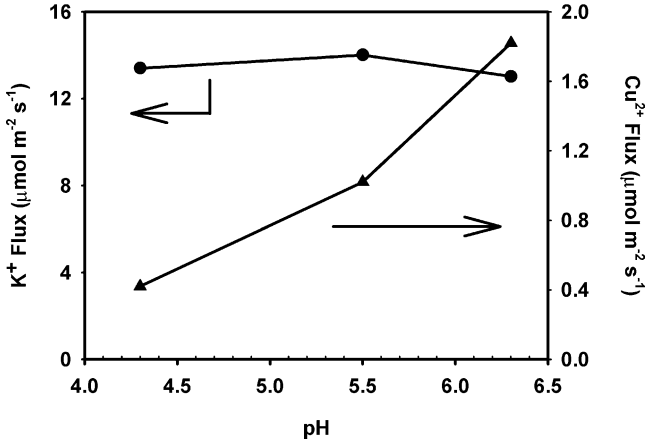

Fig. 6. K^+ and Cu^{2+} flux as function of pH. $\Delta V = 0.5$ V; $\Delta V_{bias} = -0.25$ V; $i = 0.04$–0.1 mA/cm^2. Initial concentrations: $[Cu(NO_3)_2] = 2.7$ mM (A), [KF] = 0.86 mM (B).

constant potential difference, as is shown in Fig. 6. The flux of Cu^{2+} increased with pH in the range 4.3 to 6.3. On the other hand, the flux of K^+ appeared to remain unaffected by changing pH. This is a further indication that Cu^{2+} and K^+ migrate via different transport mechanisms. There are several possible ways to explain the effect of pH on Cu^{2+} flux, and either one or a combination of reasons may hold here. The first explanation is that in addition to the observed Cu^{2+} and K^+ fluxes, there is an H^+ flux that is charge-coupled to the Cu^{2+} flux. Since the concentration of H^+ ions, which are $\sim$10 times more mobile than other anions or cations [15], increases with a decrease of pH, an increased H^+ flux may somehow suppress the flux of Cu^{2+}. An alternative explanation is that upon increasing pH the positive surface charge density of α- and γ-alumina decreases via replacement of charged OH_2^+ surface groups by chemisorption of F^- according to the net reaction $Al\text{–}OH_2^+ + F^- = Al\text{–}F + H_2O$, which occurs maximally at pH around 6 [16]. The decreased concentration of positive surface charge will lead to an increased local concentration of positive charge in the double

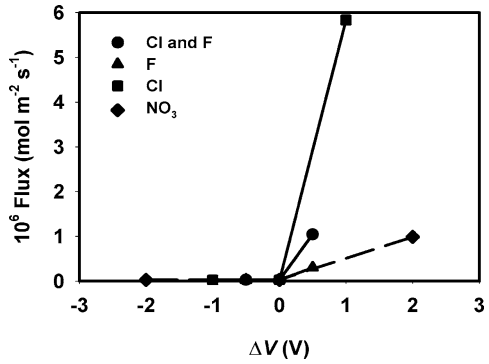

Fig. 7. Cu^{2+} flux versus ΔV as a function of electrolyte composition. (●) $[CuCl_2] = 2.3$ mM (A); [KF] = 1.8 mM (B); [KCl] = 0.2 mM (B); pH 5.5. (◆) $[Cu(NO_3)_2] = 2.0$ mM (A); $[KNO_3] = 2.0$ mM (B); pH 5.5. (■) $[CuCl_2] = 2.8$ mM (A); [KCl] = 1.3 mM (B); pH 5.5. (▲) $[CuCl_2] = 2.3$ mM (A); [KF] = 0.8 mM (B); pH 5.6.

layer of the pore, thereby promoting the transport of positively charged species (Cu^{2+}) through the pores. Third, the pH may also affect the surface charge density in the pores of the membrane directly via $Al–OH_2^+ = Al–OH + H^+$, although the alumina surface is saturated with positive charge at pH < 7 [9]. However, the effect on the permeability of positively charged species will be similar as the chemisorption of F.

3.4. Influence of electrolyte type

It was found that the composition of the electrolyte solution at constant pH and ΔV also influenced the flux of copper ions through the membrane. The influence of four electrolyte compositions on Cu^{2+} flux was determined, as shown in Fig. 7. These included KNO_3, KF, and KCl solutions and a mixture of KF and KCl. The presence of chloride in the electrolyte solution strongly promoted the flux of copper ions, while F^- and NO_3^- did not seem to have the same effect. This phenomenon can possibly be explained by chemisorption of chloride on to the gold electrodes, resulting in a negatively charged outer surface of the membrane, and the subsequent local accumulation of Cu^{2+} following Eq. (2). A similar phenomenon was reported by Martin et al. [17].

The general observation of total permselectivity toward cations under double-layer overlap conditions at pH values between 4.3 and 6.5 indicates that the mobile part of the double layer consists of positively charged ions, which in turn suggests that the interior zeta potential should be negative. This feature cannot be explained by the amphoteric behavior of the native oxide, which predicts a positive surface charge for alumina below pH 9.1 [16]. It therefore seems more likely that preferential anion adsorption occurred inside the mesopores, producing a largely immobile negative charge density. XPS analysis of several locations on a cross section of the α-Al_2O_3 support after exposure to $Cu(NO_3)_2$- and KF-containing solutions showed the presence of F and Cu (<1 at.%), as well as trace amounts of

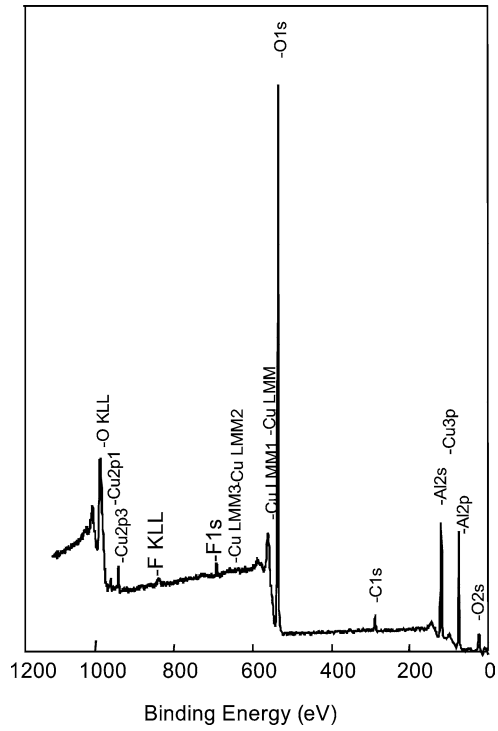

Fig. 8. XPS analysis of a cross-section of the γ-alumina layer of the membrane after transport experiments with $Cu(NO_3)_2$- and KF-containing solutions.

Ca, as is illustrated in Fig. 8. As was already mentioned, fluoride is known to adsorb specifically on α- and γ-alumina surfaces by chemisorption [16,18], and maximum uptake of fluoride occurs at pH 5–6 [16]. Under the assumption that F^- is incorporated and/or physisorbed only at the interior pore surface, the F content measured by XPS appears sufficiently high to cause a net negative fixed surface charge and explain the observed cation permselectivity. Possibly some of the F enrichment can be attributed to precipitated products such as CaF_2, while the formation of surface complexes $Al–O–M^{2+}X^-$, with M^{2+} a divalent metal cation and X^- a negatively charged anion, has also been reported [19]. XPS analysis of alumina membrane fragments after exposure to Cl^--containing solutions also indicated the presence of small amounts of Cl. Hence, a similar explanation may hold here, namely the formation of a net negative membrane surface charge due to adsorption of Cl^- inside the mesopores [5].

3.5. Influence of electrolyte strength

In Fig. 9 the influence of electrolyte concentration over a wide range of ΔV is shown. At low electrolyte concentrations the flux of Cu^{2+} is especially sensitive to changes of ΔV, while the flux of K^+ is also affected by ΔV, albeit to a lesser extent. On the other hand, at high electrolyte concentrations both anion and cation fluxes were observed. This supports the hypothesis of total permselectivity towards cations due to double-layer overlap. At ionic strengths larger

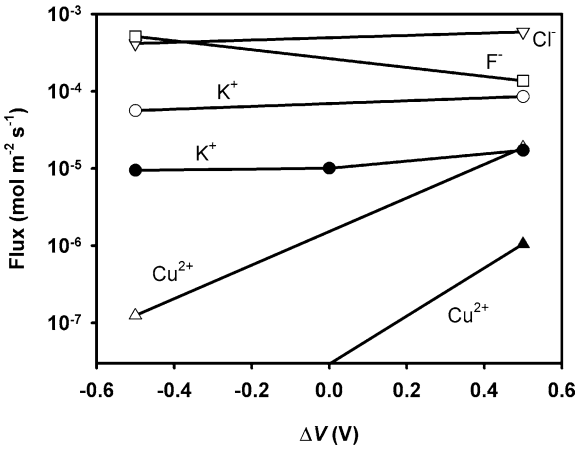

Fig. 9. Ionic fluxes versus ΔV at high and low bulk ionic strength. Closed symbols: low ionic strength; $[CuCl_2] = 2.3$ mM (A), $[KF] = 1.8$ mM (B), $[KCl] = 0.2$ mM (B); pH 5.5. Open symbols: high ionic strength; $[CuCl_2] = 0.23$ M (A), $[KF] = 0.36$ M (B), $[KCl] = 0.04$ M (B); pH 6.5. Drawn lines serve as a guide to the eye.

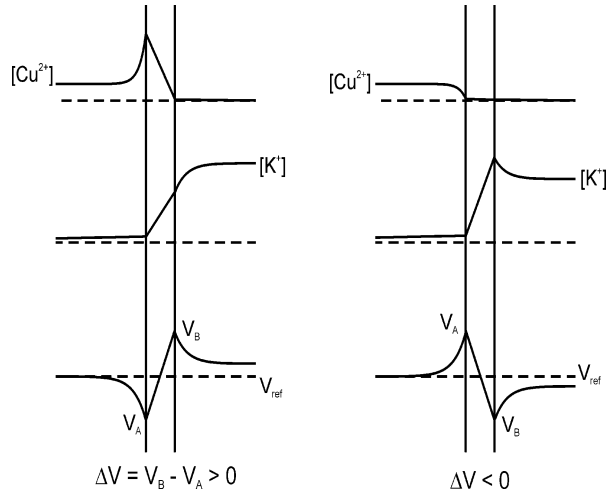

Fig. 10. Schematic diagram representing the concentration and potential profile of cations transported under electrical field conditions.

than 0.4 M, the Debye length κ^{-1} is <0.5 nm, so that the double layer is confined to a small region near the pore walls, and double-layer overlap does not occur. Since chloride and fluoride transport occur at $\Delta V = 0$, the main mode of transport of these species is Fick diffusion. However, the magnitude of these fluxes can be manipulated to some extent by variation of ΔV, and it is seen that anion transport through the membrane is promoted when the electrode with the higher potential is on the other side of the membrane, while the transport rate is suppressed when the electrode with the lower potential is on the other side of the membrane. These trends indicate that ion migration also plays a significant role in the transport of these species.

The transport behavior of K^+ can be explained as well by a combination of Fick diffusion and ion migration both at high and low electrolyte strength. But in contrast to singly charged species, higher Cu^{2+} fluxes were obtained with increasingly positive ΔV for a given feed concentration, i.e., Cu^{2+} is transported preferentially toward the electrode with the higher potential. This counterintuitive behavior may be explained by taking into account the changes of bias potential ΔV_{bias} that accompany changes of ΔV. Measured bias potentials for the experiments shown in Fig. 9 are listed in Table 1. It can be seen that ΔV_{bias} was negative when ΔV was positive, while ΔV_{bias} was positive when $\Delta V \leqslant 0$. In view of Eq. (2), a negative ΔV_{bias} will cause Cu^{2+} to accumulate near the A-side interface, while a positive ΔV_{bias} will have the reverse effect. This will alter the driving force for Fick diffusion considerably, so that much higher or lower fluxes will be observed in practice than are expected on the basis of the driving force that is calculated from the bulk concentration difference over the membrane. Monovalent species are much less sensitive to this effect. Apparently, the effect of a nonzero bias potential on the concentration difference of divalent species such as Cu^{2+} outweighs the effect of ΔV on the rate of ion migration, while it does not for monovalent species. This is illustrated in Fig. 10.

Although the cation fluxes shown in Fig. 9 increased strongly with feed concentration, the permeability of the membrane towards cations decreased with increasing ionic strength and decreasing ΔV, while the permeability of anions increased. Permeability coefficients for K^+, Cu^{2+}, Cl^-, and F^- are listed in Table 1. Here the apparent permeability P_i of species i is defined as $P_i = j_i L/\Delta c_i$, where j_i is the ionic flux, L the total membrane thickness, and Δc_i the bulk concentration difference of i over the membrane [2].

Fig. 11 shows the i–V dependence at high and low ionic strength. At low strength the i–V dependence was strongly asymmetrical around $\Delta V = 0$, while it appeared nearly symmetrical at high ionic strength. Wei et al. observed similar current-rectifying behavior at low ionic strength in quartz

Table 1
Variation of apparent ion permeability P and bias potential ΔV_{bias} with ΔV and ionic strength

Ionic strength	ΔV	ΔV_{bias}	Permeability P_i ($\text{cm}^2\,\text{s}^{-1}$)			
(mM)	(V)	(mV)	Cu^{2+}	K^+	Cl^-	F^-
2–7	0.50	−11	$(1.6 \pm 0.8) \times 10^{-5}$	$(1.9 \pm 0.2) \times 10^{-4}$	$< 2 \times 10^{-7}$	$< 2 \times 10^{-7}$
	0	41	$< 2 \times 10^{-7}$	$(1.1 \pm 0.1) \times 10^{-4}$	$< 2 \times 10^{-7}$	$< 2 \times 10^{-7}$
	−0.50	61	$< 2 \times 10^{-7}$	$(9.9 \pm 0.9) \times 10^{-5}$	$< 2 \times 10^{-7}$	$< 2 \times 10^{-7}$
400–700	0.50	−70	$(1.6 \pm 0.4) \times 10^{-6}$	$(3.6 \pm 0.9) \times 10^{-5}$	$(3.0 \pm 0.9) \times 10^{-5}$	$(2.3 \pm 0.6) \times 10^{-5}$
	−0.50	137	$(1.1 \pm 0.8) \times 10^{-8}$	$(2.7 \pm 0.7) \times 10^{-6}$	$(5.2 \pm 0.1) \times 10^{-5}$	$(9.9 \pm 0.9) \times 10^{-5}$

Experimental conditions are described in the caption of Fig. 9.

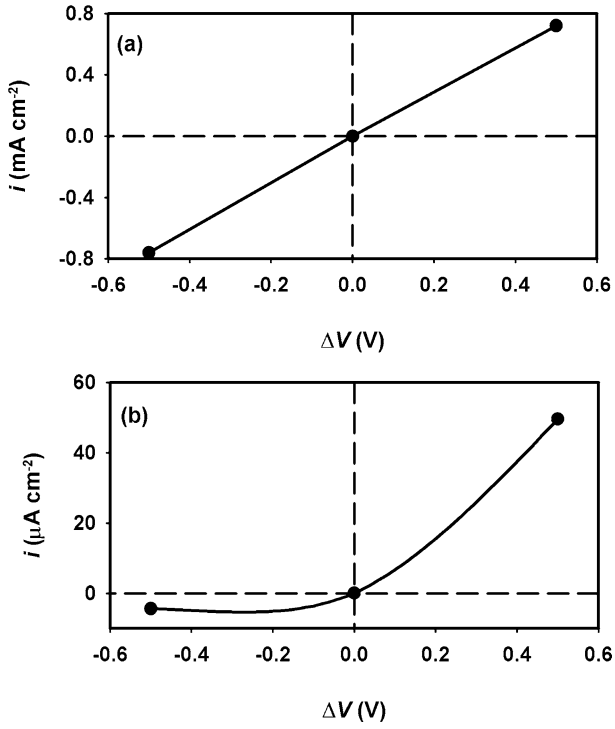

Fig. 11. Current density i versus ΔV (a) at high electrolyte strength and (b) at low electrolyte strength. Experimental conditions are described in the caption of Fig. 5.

nanopipet electrodes in KCl solutions [20]. The phenomenon was explained by a combination of double-layer overlap near the nanopipet electrode orifice and the geometric asymmetry of the orifice itself. Since double-layer overlap also occurs in γ-alumina at low ionic strength, and the γ-alumina layer has dissimilar interfaces on both sides, the i–V asymmetry observed here may be explained in a similar way. The asymmetry is most likely due to the dissimilar concentrations and electrolyte types on opposite sides of the membrane. As was shown in Fig. 9, the transport of all cations was promoted by a positive ΔV, and this is reflected by a higher current than found at negative ΔV. The symmetrical i–V behavior at high ionic strength is consistent with this explanation. Since double-layer overlap does not occur under these conditions, current rectification will not occur either.

4. Conclusions

It was shown that it is possible to control the transport rate of cations through γ-alumina membranes by variation of the potential difference over the membrane. The permeability of ions was found to be strongly dependent on the dimensions of the electrical double layer relative to the pore diameter and the sign of the applied potential. Cation permselective behavior was observed at low ionic strengths, which suggests a net negative charge density on the inner pore walls due to anion adsorption. In the absence of double layer overlap both anion and cation transport was observed. The transport mechanism of single charged ions was a combination of Fick diffusion and ion migration and the rate of transport could be controlled to some extent by variation of ΔV. The transport of doubly charged Cu^{2+} ions was found to occur mainly by Fick diffusion and could be controlled completely by variation of ΔV.

References

[1] A. van den Berg, W. Olthuis, P. Bergveld (Eds.), Micro Total Analysis Systems 2000, Kluwer, Dordrecht, 2000.
[2] P.J. Kemery, J.K. Steehler, P.W. Bohn, Langmuir 14 (1998) 2884.
[3] A. van den Berg, T.S.J. Lammerink, Top. Curr. Chem. 194 (1997) 21–50.
[4] Y. Fintschenko, A. van den Berg, J. Chromatogr. A. 819 (1998) 3–12.
[5] M. Nishizawa, V.P. Menon, C.R. Martin, Science 268 (1995) 700.
[6] T.-C. Kuo, L.A. Sloan, J.V. Sweedler, P.W. Bohn, Langmuir 17 (2001) 6298.
[7] R.J. Hunter, Foundations of Modern Colloid Science, Oxford Univ. Press, Oxford, 2001.
[8] M. Mulder, Basic Principles of Membrane Technology, Kluwer, Dordrecht, 1996.
[9] E.A. Bluhm, E. Bauer, R.M. Chamberlin, K.D. Abney, J.S. Young, G.D. Jarvinen, Langmuir 15 (1999) 8668.
[10] N. Benes, A. Nijmeijer, H. Verweij, in: N.K. Kanellopoulos (Ed.), Recent Advances in Gas Separation by Microporous Ceramic Membranes, Elsevier, Amsterdam, 2000, pp. 335–372.
[11] G.Z. Cao, J. Meijerink, H.W. Brinkman, A.J. Burggraaf, J. Membr. Sci. 83 (1993) 221.
[12] P.M. Biesheuvel, H. Verweij, J. Membr. Sci. 156 (1999) 141.
[13] For dilute solutions the driving forces exerted by the pressure and electric field gradients can be expressed as $-(v_i/k_BT)(d\Pi/dx)$ and $-(z_ie/k_BT)(dV/dx)$, respectively, with v_i the species velocity and x the direction of transport (L. Pupunat, G.M. Rios, R. Joulié, Sep. Sci. Technol. 34 (1999) 1947). Evaluation of the magnitude of these driving forces indicates that the force exerted by the electrical field is a factor of ∼1000 higher than the force exerted by the osmotic pressure.
[14] P. Trivedi, L. Axe, Environ. Sci. Technol. 35 (2001) 1779.
[15] P. Atkins, J. de Paula, Atkins' Physical Chemistry, Oxford Univ. Press, Oxford, 2002.
[16] J.L. Reyes Bahena, A. Roblero Cabrera, A. Lopez Valdivieso, R. Herrera Urbina, Sep. Sci. Technol. 37 (2002) 1973.
[17] C.R. Martin, M. Nishizawa, K. Jirage, M. Kang, S.-K. Lee, Adv. Mater. 13 (2001) 1351.
[18] Y.-H. Li, S. Wang, A. Cao, D. Zhao, X. Zhang, C. Xu, Z. Luan, D. Ruan, J. Liang, D. Wu, B. Wei, Chem. Phys. Lett. 350 (2001) 412.
[19] L.J. Crisenti, D.A. Sverjensky, Am. J. Sci. 299 (1999) 828.
[20] C. Wei, A.J. Bard, S.W. Feldberg, Anal. Chem. 69 (1997) 4627.